



ELSEVIER

Journal of Power Sources 97–98 (2001) 461–464

JOURNAL OF
POWER
SOURCES

www.elsevier.com/locate/jpowersour

EELS analysis of electrochemically deintercalated $\text{Li}_{1-x}\text{Mn}_2\text{O}_4$ and substituted spinels $\text{LiMn}_{1.6}\text{M}_{0.4}\text{O}_4$ ($\text{M} = \text{Co}, \text{Cr}, \text{Ni}$)

Youhei Shiraishi^{a,*}, Izumi Nakai^a, Koji Kimoto^b, Yoshio Matsui^b^aDepartment of Applied Chemistry, Faculty of Science, Science University of Tokyo, Kagurazaka, Shinjuku, Tokyo 162, Japan^bNational Institute for Research in Inorganic Materials, Namiki, Tsukuba, Ibaraki 304, Japan

Received 20 June 2000; accepted 13 January 2001

Abstract

Spinel lithium manganese oxides $\text{LiMn}_{1.6}\text{M}_{0.4}\text{O}_4$ ($\text{M} = \text{Mn}, \text{Co}, \text{Cr}, \text{Ni}$) for the cathode materials of the lithium ion secondary batteries were studied by electron energy loss spectroscopy (EELS). The ELNES spectra at Mn L- and O K-edge of the extracted lithium or substituted to Mn 16d site with third cations were successfully obtained. Electrochemically deintercalated $\text{Li}_{1-x}\text{Mn}_2\text{O}_4$ showed a chemical shift of both Mn L- and O K-edges to the higher energy side compared with those of the stoichiometric LiMn_2O_4 indicating oxidation of Mn and O due to the electrochemical deintercalation of Li. Substitution of M for Mn ($\text{M} = \text{Co}, \text{Cr}, \text{Ni}$) also caused a similar spectral shift of Mn L- and O K-edges. These shifts suggest lowering of the energy levels of the inner atomic orbitals compared with that of LiMn_2O_4 . © 2001 Elsevier Science B.V. All rights reserved.

Keywords: EELS; ELNES; Lithium ion batteries; Lithium manganese oxide; Spinel type structure

1. Introduction

Spinel lithium manganese oxide LiMn_2O_4 has been most expected material as a next candidate for the cathode of lithium secondary batteries [1–3]. Economically and environmentally, manganese source has advantages over LiCoO_2 . However, relatively low cycle performance and its capacity fading at high temperature operation prevent this material from expanding commercial adoption [4]. Recently, several new spinel manganates, where the Mn 16d site of the spinel structure is partially substituted by a third cation, have been studied extensively as the advanced materials. Electrochemical properties and crystal structure of these substituted materials were reported [5–11]. These materials overcome the disadvantages of stoichiometric spinel LiMn_2O_4 described above and still possess a spinel structure.

Electron energy loss spectroscopy (EELS) technique includes the near edge structure due to core loss, so-called energy loss near edge structure (ELNES), which reflects information about the unoccupied band structure about Fermi energy and electronic states of the inner atomic orbital. On the other hand, at a higher energy side of the ELNES region, extended energy loss fine structure (EXELFS) shows weak oscillation structure similarly to

EXAFS. Kurata et al. studied quantitatively chemical shifts of the Mn L- and O K-ELNES spectra for several manganese oxides with different nominal oxidation states [12]. They also examined the profiles of the spectra considering the occupation of the 3d orbital. Since EELS spectrometer and detector is equipped with transmission electron microscope (TEM), the following advantages of the TEM can be fully utilized in this technique. EELS spectrum can be obtained from a nanometer order area of a sample by using a condensed beam. The morphology of a sample can be observed in real time with fluorescent screen or CCD, whose data are recorded on a film or an imaging plate. Structural information can be obtained from the electron diffraction pattern and high resolution structure image. Chemical composition data can be obtained by EDX spectrometer. Utilizing these advantages, it is expected that EELS combined with TEM technique is powerful method to analyze electrode materials for the lithium ion batteries.

Suzuki et al. reported EELS analysis of the end members of spinel solid solutions LiMnMO_4 ($\text{M} = \text{Ti}, \text{Cr}, \text{Mn}, \text{Co}$). They clarified the valence states of manganese and other cations by comparing Mn L- and O K-ELNES spectra of the spinels with that of several standard oxides [13]. In the present study, we have applied the EELS technique to characterize the electronic states of Mn and O in electrochemically deintercalated spinel and to reveal the effect of the substitution of the third cations in the spinel lithium

* Corresponding author. Tel.: +813-3260-3662; fax: +813-3235-2214.
E-mail address: inakai@ch.kagu.sut.ac.jp (I. Nakai).

manganates $\text{LiMn}_{1.6}\text{M}_{0.4}\text{O}_4$ ($M = \text{Co}, \text{Cr}, \text{Ni}$). These materials show better cyclic performance and thermal stability than LiMn_2O_4 , and have 4V plateau that is attributable as redox reaction of $\text{Mn}^{3+}/\text{Mn}^{4+}$.

2. Experimental

Stoichiometric spinel LiMn_2O_4 and $\text{LiMn}_{1.6}\text{M}_{0.4}\text{O}_4$ ($M = \text{Co}, \text{Ni}$) and $\text{LiMn}_{1-y}\text{C}_y\text{O}_4$ ($y = 0.4, 0.7, 1.0$) were prepared by a sintering method. Electrochemical deintercalation was carried out for LiMn_2O_4 cathode. Metal lithium foil was used as the anode and 1 M $\text{LiPF}_6/\text{EC} + \text{DMC}$ as the electrolyte. The cell was charged up to 4.3 V, which led to $x \sim 1$ in formula $\text{Li}_{1-x}\text{Mn}_2\text{O}_4$. These synthesized and electrochemically treated materials were crushed in CCl_4 in an agate mortar. Then, they were spread onto carbon supporting films on copper microgrids and used as the samples for TEM/EELS study. All measurements were carried out by using HITACHI HF-3000 transmission electron microscope equipped with a cold field emission gun operated at 300 kV as an acceleration voltage. To obtain EELS spectrum, Gatan parallel EELS spectrometer was operated at 0.2 eV per channel as an energy dispersive detector. Kevex energy dispersive X-ray spectrometer was used at 10 eV per channel. First, EELS spectra of the samples were measured. Then, selected area electron diffraction pattern and EDX spectrum were taken at each sampling point in order to identify the samples as spinel $\text{LiMn}_{1.6}\text{M}_{0.4}\text{O}_4$. ELNES spectra of Mn L- and O K-absorption edges were obtained from the raw data by energy calibration and background subtraction. Zero loss and low loss spectra were also taken at each sampling point for energy calibration of ELNES spectra and estimation of the sample thickness. Energy calibration was made by using the energy of the zero loss peak. The final spectra were obtained by subtracting the extrapolated background due to the spread of the zero loss, low loss, or core loss at the lower energy.

3. Results and discussion

Fig. 1 shows a comparison of the ELNES spectra of LiMn_2O_4 with that of $\text{Li}_{1-x}\text{Mn}_2\text{O}_4$ ($x \sim 1$): Fig. 1(a) is Mn L-edge; and (b) is O K-edge spectra. The abscissa is electron energy loss due to inelastic scattering while the electron beam pass through the specimen. Total energy resolution was about 1.0 eV in the core loss edge region. The ordinate is the intensity at each channels of the energy dispersive detector. The Mn L-spectra are due to the transition from Mn 2p orbital to the unoccupied state near the Fermi energy, and O K-ELNES spectra correspond to the transition from O 1s to the unoccupied states. It is found that the white line peak of both spectra shifted to a higher energy side with electrochemical deintercalation of Li without distinct change in the shape of the spectrum. These

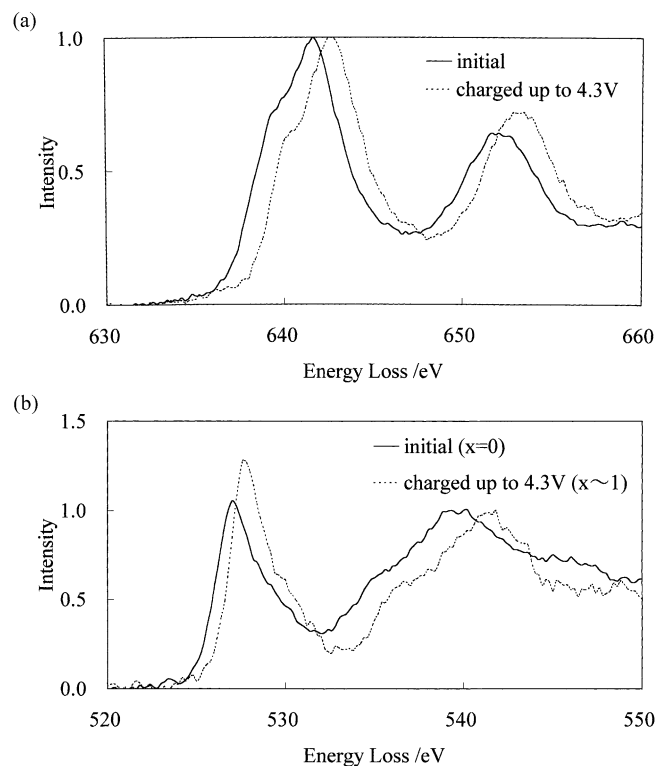


Fig. 1. (a) Mn L- and (b) O K-ELNES spectra for $\text{Li}_{1-x}\text{Mn}_2\text{O}_4$, respectively. The initial material is stoichiometric LiMn_2O_4 , and the charged material is electrochemically delithiated material with $x \sim 1$.

observations suggest that the electronic structures of Mn and O retain the initial state even after the electrochemical deintercalation. The shifts of the energy levels of the inner orbitals of Mn 2p and O 1s to lower energy are caused by decrease in the localized electron at each atom. X-ray powder diffraction analysis of these materials revealed that the lattice constant a of the cubic spinel structure decreased when lithium ion was deintercalated, and the Li deintercalation proceeded topotactically keeping the initial Mn–O framework of the spinel structure [14]. The present EELS result is consistent with the X-ray diffraction study.

Fig. 2(a) and (b) show the Mn L- and O K-ELNES spectra for $\text{LiMn}_{1.6}\text{M}_{0.4}\text{O}_4$ ($M = \text{Mn}, \text{Co}, \text{Cr}, \text{Ni}$), respectively. It is found that the substitution of Mn by the third cations cause chemical shifts of the white line peak of the Mn L-ELNES spectra. The ELNES structure of the Co, Cr and Ni edges of these spinels were also measured. A comparison of ELNES spectra with those of the standard oxides LiCoO_2 , Cr_2O_3 , and NiO , where metal atoms are octahedrally coordinated by six oxygen atoms, suggests that the Co, Cr, Ni replaced the manganese site as Co^{3+} , Cr^{3+} , Ni^{2+} ions, respectively. The chemical shift of the Mn L-edge white line peak of $\text{LiMn}_{1.6}\text{Ni}_{0.4}\text{O}_4$ from that of LiMn_2O_4 is approximately twice larger than those of $\text{LiMn}_{1.6}\text{M}_{0.4}\text{O}_4$ ($M = \text{Co}, \text{Cr}$). The average valence of Mn in the spinel manganates can be calculated from the formula $\text{LiMn}_{1.6}\text{M}_{0.4}\text{O}_4$. In our previous study using XAFS technique [15], it was clarified that the position

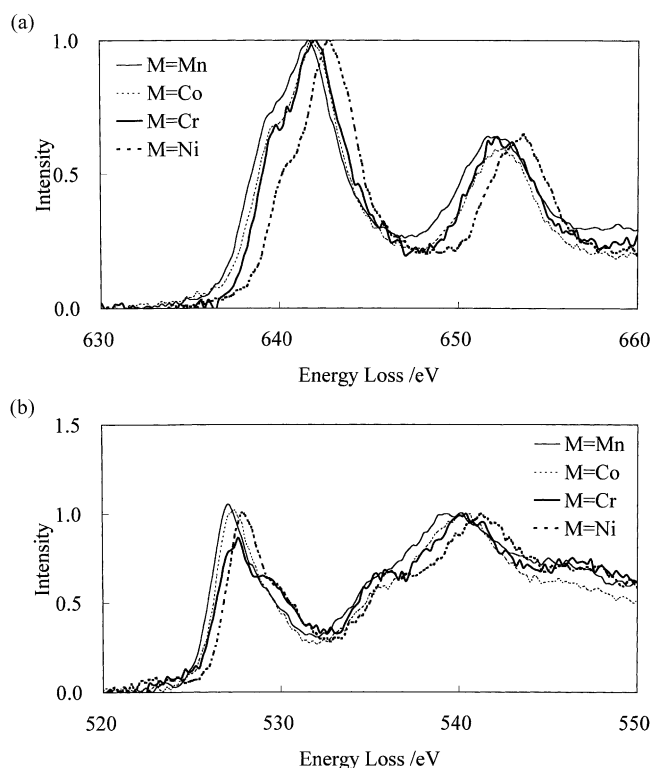


Fig. 2. (a) Mn L- and (b) O K-ELNES spectra for $\text{LiMn}_{1.6}\text{M}_{0.4}\text{O}_4$ ($\text{M} = \text{Mn}, \text{Co}, \text{Cr}, \text{Ni}$), respectively. Each material showed the electron diffraction patterns indexed with spinel structure.

of the white line peak of the Mn K-XANES spectra exhibited a linear relationship to the valence state of Mn in $\text{Li}_{1-x}\text{Mn}_2\text{O}_4$ calculated from the amount of Li. Similarly, in the Mn L-ELNES spectra, the energy of the white line peak showed an almost linear relationship with the expected Mn valency. On the other hand, the O K-ELNES spectra (Fig. 2(b)) shows chemical shifts with substitution of the cations. The linearity of the relationship between chemical shifts of the white line peak of O K-ELNES and Mn valence is similar to that of Mn L-ELNES spectra. It seems that the O atom also contributes to keep electric neutrality of the materials. A further analysis is necessary to reveal the possibility of the hole doping into the oxygen ions.

The results of X-ray powder diffraction analysis indicate that all of these substituted materials have smaller lattice constants ($a = 0.8158(4)$, $0.82120(5)$, and $0.8169(7)$) nm for $\text{M} = \text{Co}, \text{Cr}$, and Ni , respectively, than that of LiMn_2O_4 ($a = 0.8238(1)$), irrespective the ionic radii of the cation: i.e. 0.0645 , 0.0530 , 0.0545 , 0.0615 , 0.0690 nm for Mn^{3+} (high spin), Mn^{4+} , Co^{3+} (low spin), Cr^{3+} , and Ni^{2+} , respectively [16]. It seems that the decrease in the lattice constant a is due to the decrease in the octahedral Mn–O distance compared to initial stoichiometric LiMn_2O_4 . In practice, the lattice constant a is determined by several factors, i.e. a combination of the charge balance of the material by substitution with various cations and effect of their ionic radii at the octahedral 16d site of the spinel structure.

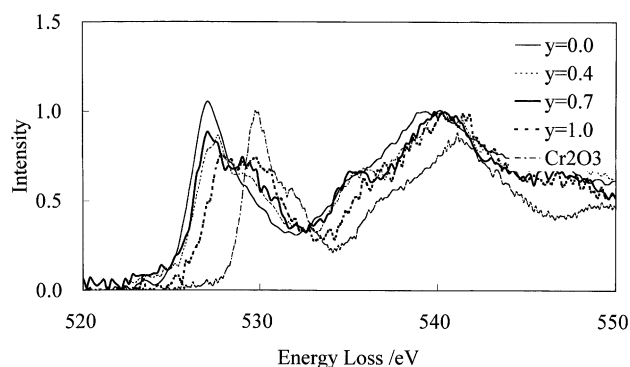


Fig. 3. Comparison of the O K-ELNES spectra of $\text{LiMn}_{2-y}\text{Cr}_y\text{O}_4$ ($y = 0.4, 0.7, 1.0$) with that of Cr_2O_3 as a standard material.

It should be noted that the O K-edge spectrum of the Cr substituted material exhibits a small shoulder peak at ca. 530 eV at the higher energy side of the white line peak at ca. 527 eV (Fig. 2(b)). In order to reveal the origin of this peak, the O K-ELNES spectra of $\text{LiMn}_{1-y}\text{Cr}_y\text{O}_4$ ($y = 0.4, 0.7, 1.0$) and Cr_2O_3 were measured and the spectra are shown in Fig. 3. The shoulder structure at the higher energy side of the white line appeared at approximately the same energy as that of the white line peak of the Cr_2O_3 of the O K-ELNES spectra. As can be seen from Fig. 3, the increase in the amount of Cr results in the enhancement of the shoulder peak followed by a decrease in the peak height of the parent white line. Therefore, the two peaks at 527 and 530 eV can be ascribed to the transitions to the p-like hybrid orbital of the Mn–O bond and that of the Cr–O bond, respectively.

4. Conclusion

EELS technique was applied for the spinel cathode materials of the lithium ion secondary batteries. This technique produces information about 10 nm order area of the sub-micron particle of a material. It was clarified that average valence of manganese and oxygen atoms increased when Mn was substituted by Co, Cr, or Ni. The decrease of the lattice constant a is caused by shrinking of the M–O₆ octahedron, irrespective the ionic radii of the third cation. A substitution of Cr for Mn in LiMn_2O_4 caused appearance of a new structure in the O K-ELNES spectra, which was assigned to be due to the Cr–O bonding interaction.

References

- [1] M.M. Thackeray, A. de Kock, W.I.F. David, *Mat. Res. Bull.* 28 (1993) 1041.
- [2] D. Guyomard, J.M. Tarascon, *Solid State Ionics* 69 (1994) 222.
- [3] R.J. Gummow, A. de Kock, M.M. Thackeray, *Solid State Ionics* 69 (1994) 59.
- [4] A. Du Pasquier, A. Blyr, P. Courjal, D. Larcher, G. Amatucci, B. Gerand, J.-M. Tarascon, *J. Electrochem. Soc.* 146 (1999) 428.
- [5] L. Guohua, H. Ikuta, M. Wakihara, *J. Electrochem. Soc.* 143 (1996) 178.

- [6] T.J. Boyle, D. Ingersoll, M.A. Rodrigues, C.J. Tafoya, D.H. Doughty, *J. Electrochem. Soc.* 146 (1999) 1683.
- [7] P. Arora, B.N. Popov, R.E. White, *J. Electrochem. Soc.* 145 (1998) 807.
- [8] Y. Gao, J.T. Dahn, *J. Electrochem. Soc.* 143 (1996) 1783.
- [9] K. Amine, H. Tukamoto, H. Yasuda, Y. Fujita, *J. Electrochem. Soc.* 143 (1996) 1607.
- [10] Q. Zhong, A. Bonakdarpour, M. Zhang, Y. Gao, J.R. Dahn, *J. Electrochem. Soc.* 144 (1997) 205.
- [11] N. Hayashi, H. Ikuta, M. Wakihara, *J. Electrochem. Soc.* 146 (1999) 1351.
- [12] H. Kurata, C. Colliex, *Phys. Rev. B* 48 (1993) 2102.
- [13] S. Suzuki, M. Tomita, S. Okada, H. Arai, *J. Phys. Chem. Solids* 57 (1996) 1851.
- [14] I.M. Kotschau, J.R. Dahn, *J. Electrochem. Soc.* 145 (1998) 2672.
- [15] Y. Shiraishi, I. Nakai, T. Tsubata, T. Himeda, F. Nishikawa, *J. Solid State Chem.* 133 (1997) 587.
- [16] R.D. Shannon, *Acta Cryst.* A32 (1976) 751.